JOURNAL OF AGRICULTURAL AND FOOD CHEMISTRY

Metabolism of Fenitrothion and Conjugation of 3-Methyl-4-nitrophenol in Tomato Plant (*Lycopersicon esculentum*)

MASAO FUKUSHIMA,* TAKUO FUJISAWA, TOSHIYUKI KATAGI, AND YOSHIYUKI TAKIMOTO

Sumitomo Chemical Co., Ltd., Environmental Health Science Laboratory, 2-1, Takatsukasa 4-chome, Takarazuka, Hyogo 665-8555, Japan

The metabolism of ^{14}C-labeled fenitrothion (Sumithion, [*O*,*O*-dimethyl-*O*-(3-methyl-4-nitrophenyl)-phosphorothioate]) in tomato plant (*Lycopersicon esculentum* Mill., cv. Ponderosa) grown in the greenhouse equipped with quartz glass was conducted to investigate the effect of sunlight on the behavior of fenitrothion and to elucidate the detailed structure of conjugated metabolites. Tomato plants (BBCH 85) were topically treated with ^{14}C-labeled fenitrothion twice with a 2 week interval between applications. At 15 days after the second application, more than half of the recovered ^{14}C was detected as unaltered fenitrothion, glucose, and cellobiose esters of 3-methyl-4-nitrophenol (NMC) in extracts from tomato fruit. The photoinduced formation of the *S*-methyl isomer of fenitrothion via thiono−thiolo rearrangement was detected only in the surface rinse but at trace amounts. In the whole tomato fruit, fenitrothion, the *S* isomer, NMC-β-glucoside, and NMC cellobioside were detected at 34.16, 1.28, 7.47, and 15.07% of the recovered ^{14}C, respectively. Trace amounts of the oxon analogue of fenitrothion were detected only on tomato leaves. The chemical structure of the cellobiose conjugate of NMC, 1-*O*-β-D-glucopyranosyl-(1→4)-β-D-glucopyranosyl-3-methyl-4-nitrophenol, was determined by spectroscopic analyses (liquid chromatography−mass spectrometry, NMR), using the metabolite obtained from leaves and stems of tomato plant hydroponically grown with ^{14}C-labeled NMC.

KEYWORDS: Fenitrothion; metabolism in *Lycopersicon esculentum*; cellobiose; glucose conjugate

INTRODUCTION

Fenitrothion (**1**) (Sumithion, *O*,*O*-dimethyl-*O*-(3-methyl-4-nitrophenyl)phosphorothioate) is an organophosphorus insecticide that has been used worldwide for forest protection and control of various plant and household insects (*1*, *2*). Although the various metabolic studies of **1** have been extensively studied in mammals (*3*), soil (*4*), and fish as well as abiotic degradation (*4*, *5*), its metabolic profiles in plants have not been fully clarified (*6*−*8*). In apple (*Malus* sp.) trees (*6*), fruits were dipped in a 0.1% emulsion of [^{14}C]-**1** labeled at the *m*-methyl group and maintained under natural weather conditions. The trace amounts of the oxon analogue of **1** and the *S*-methyl isomer of **1** were detected only on the fruit surface. 3-Methyl-4-nitrophenol (NMC) was detected in the fruit, and its glucoside and *O*-demethylated derivative of **1** were proposed as possible metabolites. Recovered ^{14}C in the fruit was higher than those on its surface after 7 days; however, about half of the radioactivity in the tissue was not fully examined. When the emulsion of ^{32}P-labeled **1** was sprayed uniformly onto the rice plants (*7*), more than half of the applied radioactivity was found to be lost due to evaporation and most of the remaining radioactivity penetrated into the plant at 10 days after the application. In the leaf blade and sheath, major degradation products were dimethylphosphorothioic, phosphorothioic, and phosphoric acids. In rice grain (*Oriza sativa* L.), **1** was rapidly degraded to the level of less than 0.01 ppm with formation of metabolites such as phosphorothioic and dimethylphosphorothioic acids at <1 ppm. A study using harvested rice grain and a postharvest treatment (*8*) proved that the *O*-demethylated derivative of **1** was the major metabolite at an early stage of incubation and NMC was formed with the lapse of time. Furthermore, in the above studies, the aglycon was supposed to be NMC, but the chemical structure of conjugated metabolites had never been identified due to usage of the limited analytical method such as gas chromatography. The ability of plants to convert the small phenolic molecules to corresponding glycosides has been extensively reviewed by Pridham (*9*). Profenofos (*O*-(4-bromo-2-chlorophenyl)-*O*-ethyl-*S*-propylphosphorothioate), with a similar structure to **1**, is mainly metabolized to 4-bromo-2-chlorophenol via ester cleavage, and its glucoside and glucosulfonyl conjugates have been confirmed from cotton extracts (*10*). The noninonic surfactant, 4-nonylphenol, has been recently reported to be converted to glucose and glucronic acid conjugates in cell cultures of wheat (*11*).

* Corresponding author.

10.1021/jf034289q CCC: $25.00
Published on Web 07/16/2003

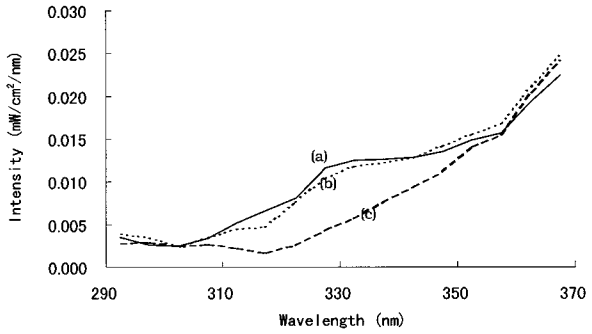

Figure 1. Spectral irradiance of sunlight outdoors (**a**), in a quartz greenhouse (**b**), and in an ordinary glass greenhouse (**c**). The sunlight intensity was measured every 5 nm for 128 times, and its average was used (Feb, 2002, noon on a clean day in Takarazuka, Japan).

Incidentally, solar irradiance (>290 nm) is known to be one of the most destructive factors for pesticides applied to plants. The transmitted sunlight through the ceiling and side glasses of a greenhouse is considered to lack much of a component at wavelengths of <370 nm due to the filtering effect of borosilicate glass (*12*) (**Figure 1**). Therefore, different degradation profiles of a pesticide in a greenhouse from those in the field may be obtained, especially when photodegradation plays a role in pesticide dissipation on the plant surface. Actually, Garau et al. (*13*) have reported the filtering effect by glass of a greenhouse on the dissipations rates of four fungicides on tomato plants under greenhouse conditions as compared with the field.

In this paper, a metabolism study of **1** in tomato plant was undertaken in a quartz greenhouse to estimate the importance of photodegradation on the plant surface and to fully elucidate the fate of **1** by the extensive spectrometric analyses.

MATERIALS AND METHODS

Chemicals. Nonradiolabeled authentic standards of **1**, its oxon derivative (**2**) [*O*,*O*-dimethyl-*O*-(3-methyl-4-nitrophenyl)phosphate], *S*-methyl isomer (**3**) [*O*-methyl-*S*-methyl-*O*-(3-methyl-4-nitrophenyl)-phosphorothiolate], *O*-demethylated derivative (**4**) [*O*-hydrogen-*O*-methyl-*O*-(3-methyl-4-nitrophenyl)phosphorothioate], carboxyl derivative (**5**) [*O*,*O*-dimethyl-*O*-(4-nitro-*m*-carboxyphenyl phosphorothioate)], NMC (**6**), and β-glucoside of **6** (**7**) [1-*O*-β-D-(glucopyranosyl)-3-methyl-4-nitrophenol] were synthesized in our laboratory according to reported methods (*5*, *14*). Uniformly labeled **1** and **6** with ^{14}C in the phenyl ring were prepared in our laboratory with specific activities of 6.66 and 29.9 MBq mg^{-1}, respectively (*15*). Their radiochemical purity was greater than 98% as determined by high-performance liquid chromatography (HPLC). Cellulase (EC 3.2.1.4) and β-glucosidase (EC 3.2.3.21) were purchased from Wako Pure Chemical Industries Ltd. (Osaka) and used for enzymatic hydrolysis of sugar conjugates to release the corresponding aglycons. Other reagents were of the purest grade commercially available.

Spectroscopy. NMR spectra were measured in D_2O with a Varian Unity-300 FT-NMR spectrometer operating at 299.94 MHz for ^{1}H and at 75.43 MHz for ^{13}C (proton decoupling) equipped with a 4-Nucleus auto NMR probe, using trimethylsilyl propionate-2,2,3,3-d_4 as an internal standard ($\delta = 0.0$ ppm). A DEPT (distortionless enhancement by polarization transfer) spectrum and, for two-dimensional NMR experiments, ^{1}H−^{1}H COSY (correlated spectroscopy), HMQC (^{1}H-detected multiple quantum coherence spectrum) (*16*), and HMBC (^{1}H-detected multiple bond heteronuclear multiple quantum coherence spectrum) (*17*) spectra were used for structural elucidation.

Liquid chromatography electrospray ionization mass spectrometry (LC-ESI-MS) in positive and negative ion modes was performed using a Thermo Finnigan TSQ Quantum spectrometer equipped with an Agilent 1100 series LC. Samples were dissolved in water or methanol and injected into an ESI source using an Agilent 1100 auto sampler at ambient temperature with a flow rate of 0.2 mL min^{-1} using a gradient system of methanol (solvent A) and 0.1% acetic acid in water (solvent B). The composition of the mobile phase was changed stepwise as follows: 0 min, %A−%B, 20:80; 0−25 min, linear, %A−%B, 30:70 at 25 min (method 1); 0 min, %A−%B, 60:40; 0−30 min, linear, %A−%B, 100; 0 at 30 min (method 2).

Radioassay. Radioactivity in the liquid extracts and the surface rinse from plants was determined by mixing each aliquot with 10 mL of Packard Emulsifier Scintillator Plus and analyzed by liquid scintillation counting (LSC) with Packard model 1600TR and 2000CA spectrometers equipped with an automatic external standard. Radioactivity in the unextractable residues from plants was measured using a Packard model 306 Sample Oxidizer. Unextractable residues were air-dried at room temperature overnight and weighed with a Mettler model AE240. Aliquots of these dried samples were subjected to combustion. $^{14}CO_2$ produced was absorbed into 9 mL of Packard Carb-CO_2 absorber and mixed with 15 mL of Packard Permafluor scintillator, and the radioactivity in it was quantified by LSC. The efficiency of combustion was greater than 90%.

Chromatography. HPLC was carried out using a Hitachi L-6200 Pump linked in series with L-4000 UV detector, D-7000 Advanced HPLC system manager, and Packard Flow-one/Beta A-120 radio detector equipped with a 500 μL liquid cell where Ultima-Flo AP (Packard) was utilized as a scintilator. A Sumipax ODS A-212 column (150 mm × 6 mm i.d. 5 μm, SCAS Co., Ltd.) was employed for both analytical and preparative purposes at a flow rate of 1 mL min^{-1}. A YMC-Pack CN A-524 column (300 mm × 10 mm i.d. 5 μm YMC Co., Ltd.) was used for a preparative purpose at a flow rate of 2 mL min^{-1}. The following gradient system was used for typical analysis of the metabolites with 0.01% trifluoroacetic acid (solvent A) and acetonitrile (solvent B): 0 min, %A−%B, 100−0; 5 min, %A−%B, 90−10; 15 min, %A−%B, 65−35; 35 min, %A−%B, 55−45; 40 min, %A−%B, 0−100; 45 min, %A−%B, 0−100; 50 min, %A−%B, 100−0 (method 3). Several HPLC methods (methods 4−6) were used for metabolite separation and purification: YMC CN A-524; 0.1% trifluoroacetic acid (solvent A) and acetonitrile (solvent B); 0 min, %A−%B, 90−10; 23 min, %A−%B, 90−10; 23.1 min, %A−%B, 0−100; 2 mL min^{-1} (method 4). Sumipax A-212; 0.1% trifluoroacetic acid (solvent A) and acetonitrile (solvent B); 0−25 min, %A−%B, 98−2, liner; 1 mL min^{-1} (method 5). YMC CN A-524; tetrahydrofuran (solvent A) and methanol (solvent B); 0−30 min, %A−%B, 95−5, liner; 2 mL min^{-1} (method 6).

Thin-layer Chromatography (TLC) was conducted using silica gel 60F_{254} thin-layer chromatoplates (20 cm × 20 cm, 0.25 mm thickness, E. Merck). The following solvent systems were used for development: toluene/ethyl acetate/2-propanol/acetic acid, 8/12/5/3 (v/v/v); chloroform/methanol, 9/1 (v/v); toluene/ethyl formate/formic acid, 5/7/1 (v/v/v). The nonradiolabeled reference standards were detected by exposing TLC plates to ultraviolet light or iodine vapor. Autoradiograms were prepared by exposing TLC plates to a BAS-IIIs Fuji Imaging Plate for several hours. The radioactivity on an imaging plate was detected by a Fuji Bio-Imaging Analyzer BAS-1500. Retention times and R_f values of compounds **1**−**7** and metabolite **1** are summarized in **Table 1**.

Plant Material, Maintenance, and Treatment. Tomato seedlings in the fourth leaf stage (*Lycopersicon esculentum* Mill., cv. Ponderosa) grown in compost (Kureha Chemical Co., Ltd., Tokyo) were transplanted to the 0.02 m^2 Wagner pot filled with either Takarazuka soil (sandy loam) or Kureha compost mixed with magnesia lime. Tomato plants were maintained in a greenhouse (June−July, 2002) equipped with a quartz glass ceiling at 25/20 °C for day/night and appropriately watered until the harvest, approximately 3 months. In the borosilicate glass greenhouse, tomato plant was grown under the same conditions to compare the photodegradation profiles of **1** on the fruit surface. Sunlight intensity around the plants in both type of greenhouses was measured with an Ushio Spectroradiometer USR-20B.

For the investigation of metabolic profiles, [^{14}C]-**1** in the following solutions was topically applied at rates of 75 and 750 g a.i. ha^{-1} to the fruits and leaves of tomato plants grown in a quartz glass greenhouse twice with a 2 week interval. In the case of a borosilicate glass greenhouse, a similar application was conducted only for tomato fruits at 750 g a.i. ha^{-1}. For preparation of the dosing solution, 0.362 mg of [^{14}C]-**1** was dissolved in 1.45 mL of acetonitrile (1.67 MBq mL^{-1}). In

the case of the leaf treatment, 0.54 mg of [^{14}C]-**1** was isotopically diluted in 4.32 mL of acetonitrile by 2-fold with the same amount of nonradiolabeled **1** (0.83 MBq mL^{-1}). The surface area (cm^2) of the fruit just before each application was calculated to be 50.3 cm^2 from its radius (2 cm) by assuming a spherical shape. The surface area of the leaf was geometrically estimated to be 10 cm^2 per leaf on average. The application rate to the surface of tomato fruits and leaves was calculated as 3 μL per unit area; therefore, 150.9 and 30 μL of the prepared solution were topically applied with a microsyringe to each surface, respectively. A total of four fruits and 30 leaves were used. The first application was conducted at the fruit growth stage (BBCH 85), and the preharvest interval (PHI) was set as 15 days.

For the purpose of collecting enough amount of conjugated metabolites subjected to spectroscopic analyses (MS, NMR), tomato seedlings (*L. esculentum* Mill., cv. Ponderosa, BBCH 12) were hydroponically grown in an aqueous solution of [^{14}C]-**6**. The petiole of an excised leaf was placed into a 20 mL bottle filled with the aqueous solution of isotopically diluted [^{14}C]-**6** 100-fold with nonradiolabeled compound at a concentration of 11.9 mg L^{-1} (1/100 of water solubility of NMC, 1188 ppm (*18*)). The bottles were sealed with a semitransparent thermoplastic film, covered with aluminum foil, and kept in the same greenhouse used in the metabolism study. The leaves were sampled at 10 and 17 days after treatment and extracted for metabolite studies.

Extraction and Isolation of Metabolites. Tomato fruits applied with [^{14}C]-**1** were sampled at 15 days after the second treatment. The harvested samples were weighed and stored in a freezer (<−20 °C) until analysis was conducted. After the surface was rinsed with methanol (50 mL per fruit), tomato fruits were extracted with acetone/water (4/1,v/v, 300 mL) using a Nissei Excel Auto homogenizer (10 000 rpm, 10 min at 0 °C) and then, the homogenate was filtered. In the case of the borosilicate glass greenhouse experiments, only the surface rinse with methanol was conducted. This extraction procedure was repeated twice in the same manner, and the extracts were combined. The aliquots of surface rinse and extract were individually radioassayed with LSC and analyzed by HPLC and TLC. Pulp residues were air-dried in open vessels at room temperature overnight, and subsamples of dried residues were subjected to combustion analysis to determine the remaining radioactivity.

Tomato leaves treated with [^{14}C]-**1** were also sampled at 15 days after the second treatment. The surfaces of the tomato leaves were rinsed with methanol (10 mL per leaf), extracted, and analyzed in the same manner as the treated fruits.

Untreated fruits and leaves of the test plants were also sampled to examine the extent of ^{14}C translocation. They were chopped, air-dried in chamber at room temperature for 1 week, and subjected to combustion.

The leaves uniformly treated with [^{14}C]-**6** were removed from the hydroponic solution after 10 or 17 days of exposure and extracted in the same way as described above without conducting any surface rinse. The extracts were concentrated and nearly dried by rotary evaporation under reduced pressure, dissolved in 10 mL of distilled water, and successively partitioned with 10 mL of hexane. The water layer was subjected to column chromatography with 80 g of Sephadex LH-20 conditioned with methanol, and eluates by methanol were collected with an Advantec SF-2120 fraction collector. The fractions containing the radioactivity were combined and subjected to solid phase extraction with Waters Sep-pak C18, which was conditioned with 5 mL of methanol following 10 mL of distilled water. The extract was applied to a Sep-pak cartridge and successively eluted with 10 mL of distilled water and 10 mL of a mixture of methanol and distilled water (2/8, v/v) and finally with 10 mL of methanol. The eluates from the mixture solvent were combined and concentrated and then subjected to the repeated purification using by HPLC (methods 3−6).

Identification of Metabolites. The identification of **1** and its metabolites was conducted by HPLC and two-dimensional (2D) TLC cochromatography with nonradiolabeled reference standards. The major polar metabolite that did not match with any reference standard by simple HPLC and 2D TLC cochromatography was first subjected to both enzymatic hydrolysis (cellulase and β-glucosidase, 37 °C, 12 h) in 10 mM phosphate buffer at pH 5 and acidic hydrolysis (1 M HCl, 80 °C, 2 h) to examine the profiles of conjugates (*19*). Acetylation was conducted by treating the isolated metabolite with anhydrous acetic acid in the presence of trace dry pyridine according to the usual manner (*20*, *21*). Second, the major unknown metabolite isolated from extracts of seedlings treated with [^{14}C]-**6** was subjected to LC-ESI-MS and NMR analyses.

Table 1. Retention Times (HPLC) and R_f Values (TLC) of Reference Compounds and Metabolite **1**

compd	retention time	R_f value (min) system 1[a]	system 2[b]	system 3[c]
1	44.6	0.78	0.71	0.73
2	28.8	0.64	0.60	0.52
3	33.1	0.68	0.63	0.54
4	19.8	0.29	0.00	0.14
5	34.1	0.65	0.02	0.54
6	26.9	0.73	0.38	0.59
7	18.6	0.29	0.02	0.08
metabolite **1**[d]	16.9	0.05	0.00	0.00

[a] Toluene/ethyl acetate/2-propanol/acetic acid = 8/12/5/3 (v/v/v/v). [b] Chloroform/methanol = 9/1 (v/v). [c] Toluene/ethyl formate/formic acid =5/7/1 (v/v/v). [d] Metabolite **1**.

RESULTS

Sunlight Conditions. The spectral irradiance of sunlight reaching the plant surface of tomato plants was measured in the greenhouse equipped with a quartz (**Figure 1b**) or an ordinary borosilicate glass (**Figure 1c**) ceiling, respectively, and was compared with that of natural sunlight measured outdoors in February, 2002 (**Figure 1a**). The sunlight irradiance at wavelengths between 300 and 360 nm in the quartz greenhouse was very close to that measured outdoors, while the spectrum with a cutoff of about 320 nm was obtained in the greenhouse equipped with the borosilicate glass. Because **1** has a measurable absorption tail at a wavelength greater than 290 nm (*4*), these differences of light conditions are likely to affect photodegradation of **1** on plant surfaces.

Distribution of Metabolites. In the case of the treatment in quartz glass greenhouse at a dose of 75 g a.i. ha^{-1}, the recovered radioactivity was 36.4 and 66.9% of the nominally applied ^{14}C in the tomato fruit and leaf applications, respectively. In the treated tomato fruit experiment, only 1.54% of total radioactive residue (% TRR) (0.0016 ppm) and 1.15% TRR (0.0012 ppm) remained in the untreated leaf and untreated fruit, respectively. In the case of the tomato leaf treatment, only 0.98% TRR (0.06 ppm) remained in the untreated leaf, with no radioactivity in the untreated fruit. These results indicate that the translocation of radioactivity from the treated portions to others is few and the unrecovered ^{14}C is likely to be lost by vaporization at harvest.

The distribution of radioactivity and metabolites in the surface rinse, extracts, and bound residues in tomato fruit treated with [^{14}C]-**1** at a dose of 75 g a.i. ha^{-1} is summarized in **Table 2**. Approximately 60% TRR was detected in the extract, and the remaining ^{14}C was on the surface and in the unextracted residue. In the surface rinse, most ^{14}C occurred as **1** with a trace amount of **3**, but neither **2**, **4**, nor **5** were detected. In the extract, major components were **1** and **7** and metabolite **1**. Compound **1** was a major residue (32.7% TRR, 0.035 ppm) within the whole tomato fruit and **3**, **7**, and metabolite **1** amounted to 1.2 (0.001 ppm), 7.2 (0.008 ppm), and 14.4% TRR (0.015 ppm), respectively. Meanwhile, the distribution of radioactivity from the treated leaves was different from that of the fruit. Approximately 75 and 22% TRR were recovered from the surface rinse and

Table 2. Distribution of Radioactivity and Metabolites in Each Treatment of [^{14}C]-**1** to the Fruits and Leaves

	fruit				leaf			
	75 q a.i.ha^{-1}		750 q a.i.ha^{-1}		75 a a.i.ha^{-1}		750 q a.i.ha^{-1}	
component	% TRR	ppm[a]	% TRR	ppm[a]	% TRR	ppm[a]	% TRR	ppm[a]
				surface				
1	18.3	0.02	85.2	3.79	70.9	4.33	87.8	76.21
2	ND	ND	ND	ND	0.4	0.02	0.5	0.41
3	1.2	<0.01	ND	ND	2.4	0.14	1.1	0.98
4	ND	ND	ND	ND	ND	ND	ND	ND
5	ND	ND	ND	ND	ND	ND	ND	ND
6	ND	ND	ND	ND	0.4	0.03	ND	ND
7	ND	ND	ND	ND	ND	ND	ND	ND
metabolite **1**	ND	ND	ND	ND	ND	ND	ND	ND
others	1.07[b]	<0.01	ND	ND	0.93[b]	0.06	ND	ND
				extract				
1	14.4	0.02	5.4	0.24	6.2	0.38	6.0	5.22
2	ND	ND	ND	ND	ND	ND	ND	ND
3	ND	ND	ND	ND	ND	ND	ND	ND
4	NMD	ND	ND	ND	ND	ND	ND	ND
5	ND	ND	ND	ND	ND	ND	ND	ND
6	ND	ND	ND	ND	0.7	0.04	1.1	0.94
7	7.2	<0.01	ND	ND	0.7	0.04	ND	ND
metabolite **1**	14.4	0.02	ND	ND	8.0	0.49	0.3	0.24
others	20.62[c]	0.02	2.72[d]	0.12	6.19[e]	0.38	1.67[f]	1.45
unextractable	20.1	0.02	6.4	0.29	2.4	0.14	1.4	1.21
untreated leaf	1.5	<0.01	0.2	<0.01	1.0	0.06	0.2	0.18
untreated fruit	1.2	<0.01	0.1	<0.01	ND	ND	ND	ND
total	100.0	0.11	100.0	4.45	100.0	6.11	100.0	86.84

[a] ppm of 1 equiv. [b] Consisted of two components with almost the same amounts. [c] Seven polar components, each less than 6.60% TRR (<0.01 ppm). [d] Three polar components, each less than 2.47% TRR (0.11 ppm). [e] Three polar components, each less than 3.99% TRR (0.24 ppm). [f] Three polar components, each less than 1.38% TRR (1.20 ppm).

the leaf extract, respectively, with the remaining ^{14}C in the unextracted residue. In the surface rinse, most of the radioactivity was unaltered **1** and only trace amounts of **2**, **3**, and **6** were detected. In the extract, **1**, **6**, **7**, and metabolite **1** were detected. In total, **1** was a major residue, amounting to 77.0% TRR (4.704 ppm). These results indicated more penetration of **1** followed by metabolic degradation in tomato fruits as compared with leaves. The photoinduced formation of **3** was observed as a minor pathway in both treatments but the oxidation of **1** to **2** occurred also on leaves as a minor pathway. In the borosilicate glass greenhouse experiment, **1** amounted to 84.1% of recovered radioactivity from the surface of tomato fruits as a main component with small amounts of polar metabolites (<10.3% TRR) but neither **2** nor **3** was detected.

The metabolic profiles in tomato leaves treated at a higher dose rate of 750 g a.i. ha^{-1} were nearly the same as those of 75 g a.i. ha^{-1} except for slight differences in the ^{14}C distribution. On the other hand, in the case of tomato fruits, the metabolic profiles differed from the rate of 75 g a.i. ha^{-1}. Most of the recovered ^{14}C was on the surface, and only 8.1% TRR was recovered from the extract. With the whole fruit, **1** was the main residue (90.6% TRR) and **2**−**5**, **7**, and metabolite **1** were not detected at all.

Identification of Metabolite 1. From the excised leaves of tomato seedlings treated with [^{14}C]-**6**, **6** (37.9%) and metabolite **1** (41.0%) were collected from the extract as major residues. Metabolite **1** obtained from excised leaves was confirmed to be identical with that obtained from the intact tomato fruit by HPLC (method 1) and 2D TLC cochromatography.

To characterize the conjugation profile, metabolite **1** isolated from the extracts was first subjected to the various types of hydrolysis. It was almost quantitatively hydrolyzed to **6** by 1 M hydrochloric acid under the tested conditions, as demonstrated by 2D TLC and HPLC cochromatography with reference standard. The treatment with cellulase or β-glucosidase also resulted in the almost complete conversion of metabolite **1** to **6**, while no conversion was observed without enzymes. These results strongly suggested that the metabolite **1** is a sugar conjugate of **6**.

Second, metabolite **1** was subjected to spectroscopic analyses. Its mass spectrum obtained in a negative ion mode (method 1) is shown in **Figure 2**. The $[M - H]^-$ ion was observed at *m*/*z* 476 together with an adduct ion $[M + CH_3COO]^-$ at *m*/*z* 536 and $[M - 2\text{glucose} - H]^-$ at *m*/*z* 152. This fragment ion implied that the metabolite **1** molecule contained two carbohydrate moieties and **6** (*m*/*z* 152). The mass spectrum in the positive ion mode (method 2) of the acetylated metabolite **1** exhibited a peak at *m*/*z* 772 corresponding to $[M + H]^+$, which indicated the presence of seven acetate groups. The following ions were observed from measurement in a product ion mode at *m*/*z* 772 (**Figure 3**): *m*/*z* (ion), 772 ($[M + H]^+$), 619 ([M − (3-methyl-4-nitrophenol) + H]$^+$), 440 ([M − tetraacetylglucose + H]$^+$), 331 ([tetraacetylglucose] $^+$).

The ^{1}H NMR (300 MHz, D_2O, δ) spectrum of metabolite **1** showed the presence of 12 carbohydrate protons with one methyl group (2.61 ppm) and three aromatic ring protons (7.13 and 8.13 ppm) (**Table 3**). Although many signals derived from the carbohydrate protons were overlapping at 3.2−4.2 ppm, where the bulk of carbohydrate protons are observed (*22*), two anomeric protons (4.48 ppm, $J = 7.2$ Hz; 5.24 ppm, $J = 7.5$ Hz) were clearly separated from others and detected at a lower field. The ^{13}C NMR (75 MHz, D_2O, δ) spectrum of metabolite **1** indicated the presence of one methyl group (23.34 ppm), six aromatic carbons (117.07, 122.53, 130.44, 140.43, 146.26, and 162.80 ppm), 10 carbons connected to an oxygen atom (63.55, 71.23, 72.06, 72.50, 75.58, 75.98, 78.17, 78.29, 78.56, and 78.76 ppm), and two carbons connected to two oxygen atoms (102.08 and 105.55 ppm). The HSQC spectrum and ^{1}H−^{1}H COSY were

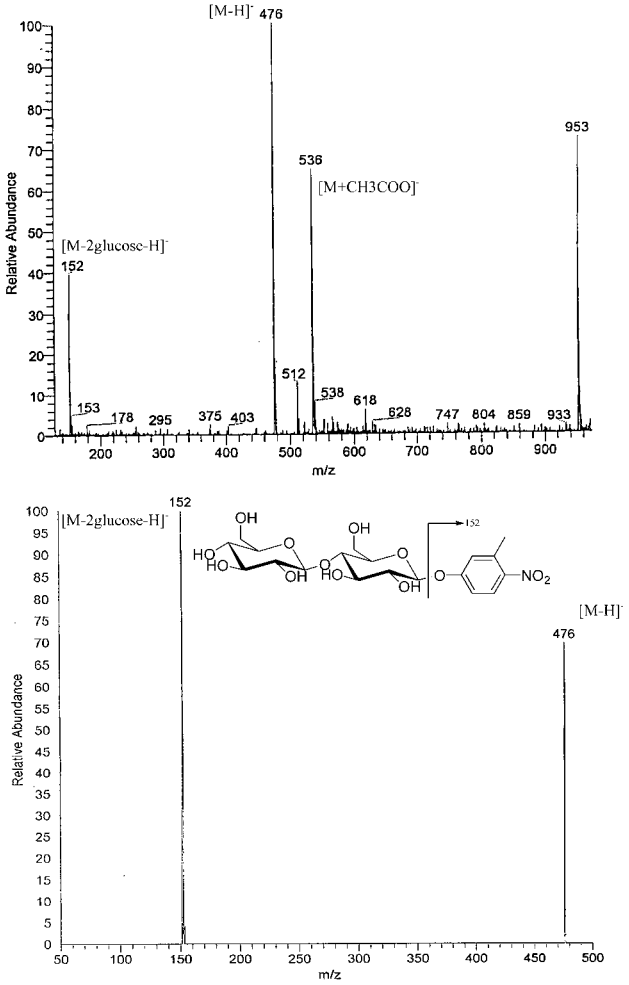

Figure 2. Mass spectra of metabolite **1** in a negative ion mode; mass spectrum in a full scan mode (upper) and a product ion mode of *m*/*z* = 476 (lower).

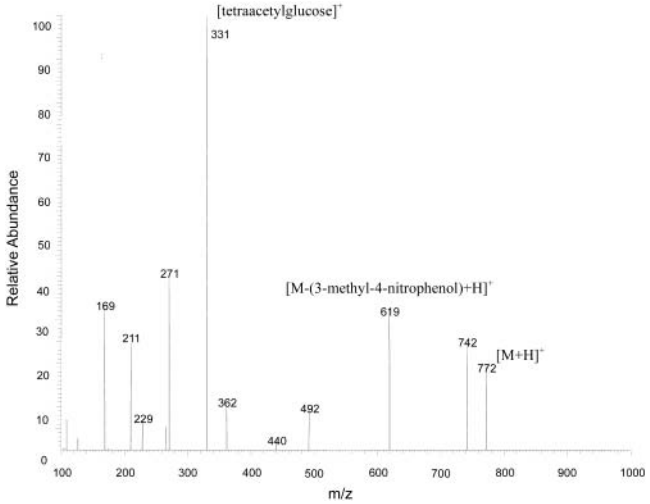

Figure 3. Mass spectra of acetylated metabolite **1** in a product ion mode of *m*/*z* = 772.

also measured to determine the identity of the ^{13}C and ^{1}H signals obtained. The detailed assignment of structure information on disaccharide was defined by the HMBC experiment. Cross-peaks due to long-range correlations were observed between C-4 of glucose, which attaches to the aromatic ring (71.23 ppm), and H-1 of the other glucose (4.48 ppm); C-1 of glucose, which

Table 3. Chemical Shifts of Metabolite **1** in Deuterium Oxide (99.98%-*d*)

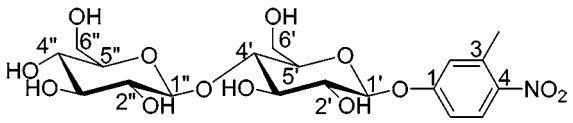

position	^{1}H	^{13}C
l		162.8
2	7.13 (brs)	122.5
3		140.4
3-CH_3	2.61 (s)	23.3
4		146.3
5	8.13 (brd, 9.6)	130.4
6	7.13 (brs)	117.1
1′	5.24 (brd, 7.5)	102.8
2′	3.64 (m)	76.0
3′	3.90 (m)	63.6[a]
4′	4.22 (brd)	71.2[a]
5′	3.90 (m)	78.1[a]
6′	3.64 (m)	78.6[a]
	3.36 (m)	
1″	4.48 (d, 7.2)	105.5
2″	3.34 (m)	78.8
3″	3.34 (m)	72.0[a]
4″	3.34 (m)	72.5[a]
5″	3.64 (m)	75.6[a]
6″	3.64 (m)	78.3[a]
	3.90 (m)	

[a] These overlapping signals may be interchangeable between two sugar moieties.

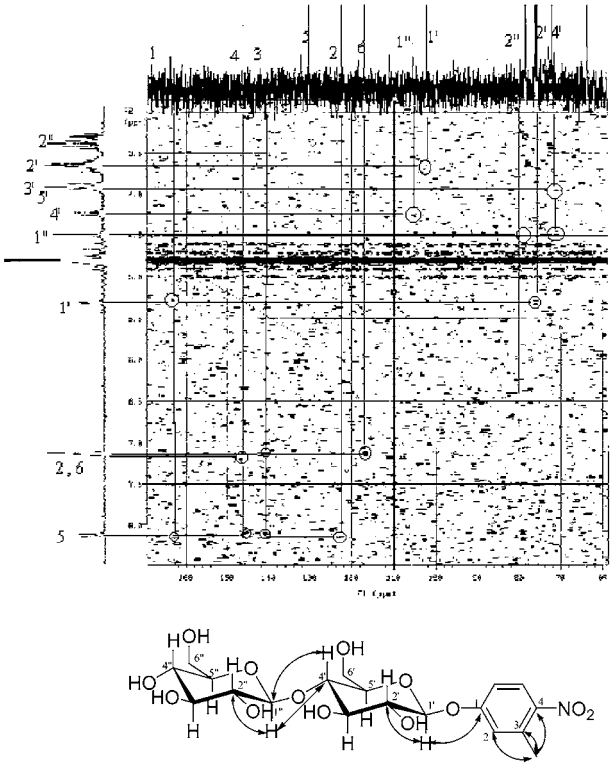

Figure 4. HMBC correlations of metabolite **1**.

attaches to the aromatic ring (105.55 ppm), and H-1 of the other glucose (4.22 ppm); and C-1 of aglycon (162.80 ppm) and H-1 of glucose, which attaches to aromatic ring (5.24 ppm) (**Figure 4**). These results clearly indicate that metabolite **1** is 1-*O*-*β*-D-glucopyranosyl-(1→4)-*β*-D-glucopyranosyl-3-methyl-4-nitrophenol. On the basis of these results, the metabolic pathway of **1** in tomato plants is proposed (**Figure 5**).

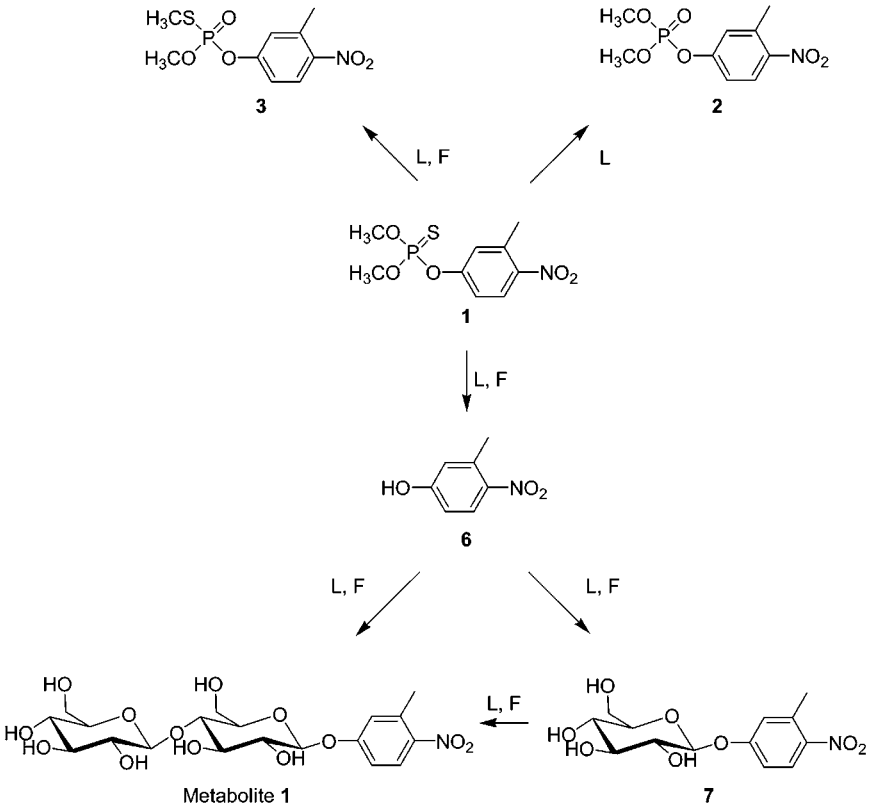

Figure 5. Proposed metabolic pathway of **1** in the tomato plant (L, on leaf surface; F, in fruit tissue).

DISCUSSION

Upon application of **1** to tomato plants, **1** is considered to first undergo photodegradation in epicitícular wax with concomitant penetration into plant tissues followed by various types of metabolic conversion. The typical photoreactions of **1** are known to be oxidation of the P═S moiety and/or aryl methyl group in the presence of molecular oxygen and thiono−thioro rearrangement of the *O*-methyl group to the P═S sulfur atom (*4*, *15*, *23*). In the case of parathion, Schwack et al. have recently reported the photoreaction of the nitro group leading to formation of the corresponding azo-, azoxy-, and 2-hydroxyazo-dimers by using the enzymatically isolated green paprika cuticles or the cutin acid 12-hydroxystearic acid (*24*, *25*).

Because the tail of UV absorption of **1** is known to extend over 290 nm, the spectral irradiance of sunlight in the greenhouse is important to understand the possible contribution of these photoreactions. As evidenced from **Figure 1**, **1** is most likely to be subjected to the same sunlight photodegradation as occurs outdoors although the temperature conditions are controlled. The rearrangement of the *O*-methyl group to form **3** proceeds both thermally at >120 °C and photochemically (*26*), but the latter process is most probable in the metabolism study. In our study, **3** was formed on both fruits and leaves of tomato plants grown in the quartz glass greenhouse but not in the borosilicate glass one, indicating the importance of light at 290−350 nm transmitted through quartz glass. Photooxidation to form the oxon derivative is one of the common reactions of organophosphorus pesticides such as parathion (*27*), cyanox (*28*), and bromophos (*29*). Compound **2** was detected on tomato leaves in a trace amount as similarly observed in previous studies using bean (*5*), rice leaves (*7*), and apple fruits (*6*), but it was not formed on tomato fruits. The amount and component of epicuticular wax vary significantly with plant species. Leaves of rice, bean, and tomato plants have very small amounts of waxes (0.4−7.3 μg cm^{-1}) (*30*−*32*), while extremely more amounts (20−1000 μg cm^{-1}) have been reported for tomato and apple fruits and depend on the growing stage (*33*, *34*). The main components of tomato epicuticular wax are C_{28}−C_{34} hydrocarbons, and the amounts of triterpenols such as amyrin increase as fruits ripen. Both light and oxygen molecules are considered indispensable to the formation of **2** (*23*); therefore, the photoinduced oxidation would proceed more easily in the thinner wax layers of bean, rice, and tomato leaves. The thicker wax layer could prevent **1** from reacting with molecular oxygen, which is the case for the present study. However, **2** was formed on the surface of apple fruits, which may be suggested by the presence of aldehydes and ketones as wax components in apples usually acting as a photosensitizer. Because the rearrangement of **1** to **3** proceeds only by absorption of light, formation of **3** was considered to be less sensitive to wax thickness. The formation of **5** has been reported to require photoexcitation of **1**, causing intramolecular hydrogen abstraction by the nitro group from the adjacent methyl group, followed by the successive reactions of molecular oxygen with the *aci*-nitro intermediate formed (*23*). If the reaction environment forming **5** is similar to that for **2**, **5** should be detected on a plant surface with a thinner wax layer. By the way, the radical intermediate is most probably involved in the formation of **5** and the wax components usually possess the unsaturated acyclic and cyclic moieties (*25*, *35*). Therefore, the radical precursor of **5** is likely to be trapped by these wax components, resulting is less detection of **5**. In actuality, a trace amount of **5** (0.1−0.4%) has been detected only on bean leaves (*5*). As for the complex azo- and azoxy-dimers reported as dominant degradates of parathion on green paprika cuticles (*25*), the HPLC chromatograms of fruit and leaf extracts in our study did not show any unknown peaks corresponding to such nonpolar degradates. The related metabolism studies have been conducted under the different conditions, and it is impossible to simply explain the differences in dissipation of **1** on plant surfaces by a simple

factor, but the characteristics of epicuticular waxes seem, at least in part, to account for the different photodegradation of **1** on tomato plant surfaces.

After penetration into the plant tissues, **1** is considered to undergo various metabolic degradation steps. Ester cleavage followed by conjugation of the corresponding phenol with sugar is the most familiar process, as well as demethylation of the *O*-methyl group (*36*). *O*-Demethylation is one of the main metabolic pathways for organophosphorous pesticides. Compound **4** was detected in apple fruit in a trace amount (*6*) but could not be found in rice (*7*) and tomato plant (this study), indicating that this process is minor in those plants. In the present study, **6** amounting to 2.6% TRR was detected in tomato leaves, indicating the involvement of ester cleavage in metabolism. Although **6** was absent in tomato fruits, the corresponding sugar conjugates, **7** and metabolite **1**, were instead detected. Incidentally, the previous metabolism studies of other pesticides in tomato plants show the formation of various sugar conjugates including simple glucoside, disaccharides, and malonyl glucosides. The simple *O*-glucosides were reported for clomazone (*37*), oxamyl (*38*), baythroid (*39*), and diphenamide (*40*); hence, the detection of **7** in the present study showed that this conjugation is very similar in tomato fruits. In contrast, this conjugate was detected in tomato leaves at trace amounts suggesting that a lower amount of relevant enzymes exists therein. The conjugation with di- and trisaccharides as well as 6-*O*-malonylglucose is widely known for metabolism of various pesticides in tomato (*41*). Schmidt extensively investigated the sugar conjugates of 4-nitrophenol formed parathion in cell suspension cultures of the several plant species and identified glucoside, galactoside, malonylated glucoside, and gentiobioside as carbohydrate moieties (*42*). The mechanism of glycosylation has been investigated, and diglucosides were supposedly formed by stepwise addition of a glucose unit to the first glucose ester; pentosylation and malonylation would prevent further extension of saccharide chains. Because the chemical structure of **1** is similar to that of parathion, it is likely that a similar conversion mechanism operated in the metabolism of **1** in tomato plant leading to formation of **7** and metabolite **1**. The significant formation of those conjugates in fruits with a trace amount of only metabolite **1** detected in leaves may imply that stepwise glucosylation is the characteristic metabolic process in fruit and that part of these polar metabolites is translocated to leaves through phloem. In the fruit applications of **1** at the higher rate, neither **6** nor its conjugated metabolites was scarcely detected, while the trace amount of metabolite **1** was present in the leaf applications. It may be considered that the excess amount of **1** precipitates in the thicker wax layer of tomato fruits and much less **1** is available for penetration and metabolic conversion. In contrast, the wax layer in leaves is much thinner; hence, **1** might partly penetrate into the tissues and be metabolized.

LITERATURE CITED

(1) Hattori, J.; Oizumi, K.; Sato, Y.; Tsuda, K.; Abe, T.; Harada, M. Biologocal properties of Sumithion. *Residue Rev.* **1976**, *60* (39), 39−82.

(2) Phillips McDougall, Products Section-Market, 1999−2002.

(3) Mihara, K.; Okuno, Y.; Misaki, Y.; Miyamoto, J. Metabolism of fenitrothion in goats. *J. Pestic. Sci*. **1978**, *3*, 233−242.

(4) Mikami, N.; Imanishi, K.; Yamada, H.; Miyamoto, J. Photodegradation of fenitrothion in water and on soil surface, and its hydrolysis in water. *J. Pestic. Sci*. **1985**, *10*, 263−272.

(5) Ohkawa, H.; Mikami, N.; Miyamoto, J. Photodecomposition of sumithion [O,O-Dimethyl-O-(3-methyl-4-nitrophenyl)phosphorothioate]. *Agric. Biol. Chem*. **1974**, *38* (11), 2247−2255.

(6) Hosokawa, S.; Miyamoto, J. Metabolism of ^{14}C-labeled sumithion, O,O-dimethyl-O-(3-methyl-4-nitrophenyl)phosphorothioate in apple. *Botyu Kagaku* **1974**, *39*, 49−53.

(7) Miyamoto, J.; Sato, Y. Determination of insecticide residue in animal and plant tissues II. *Botyu Kagaku* **1965**, *30*, 45−49.

(8) Takimoto, Y.; Ohshima, M.; Miyamoto, J. Degradation and fate of fenitrothion applied to harvested rice grains. *J. Pestic. Sci*. **1978**, *3*, 277−290.

(9) Pridham, J. B. The phenol glucosylation reaction in the plant kingdom. *Phytochemistry* **1964**, *3*, 493−497.

(10) Capps, T. M.; Barringer, V. M.; Eberle, W. J.; Brown, D. R.; Sanson, D. R. Identification of a unique glucosyl sulfate conjugate metabolite of profenfos in cotton. *J. Agric. Food Chem.* **1996**, *44*, 2408−2411.

(11) Bokern, M.; Nimtz, M.; Harms, H. H. Metabolites of 4-*n*-nonylphenol in wheat cell suspension cultures. *J. Agric. Food Chem.* **1996**, *44*, 1123−1127.

(12) Kleier, D. A. Environmental effects on the photodegradation of pesticides. *BCPC Monogr*. **1994**, *59*, 97−109.

(13) Garau, V. L.; Angioni, A.; Real, A. A. D.; Russo, M.; Cabras, P. Disappearance of azoxystrobin, pyrimethanil, cyprodinil, and fludioxonil on tomatoes in a greenhouse. *J. Agric. Food. Chem.* **2002**, *50*, 1929−1932.

(14) Greenhalgh, R.; Marshall, W. D. Ultraviolet irradiation of fenitrothion and the synthesis of the photolytic oxidation products. *J. Agric. Food. Chem.* **1976**, *24* (4), 708−713.

(15) Yoshitake, A.; Kawahara, K.; Kamada, T.; Endo, M. Labeled organophosphorus pesticides I. synthesis of carbon-14 labeled *O*,*O*-dimethyl *O*-(3-methyl-4-nitrophenyl) phosphorothioate (Sumithion). *J. Labelled Compd. Radiopharm.* **1976**, *13*, 323−331.

(16) Summers, M. F.; Marzilli, L. G.; Bax, A. Complete ^{1}H and ^{13}C assignments of coenzyme B_{12} through the use of new two-dimensional NMR experiments. *J. Am. Chem. Soc.* **1986**, *108*, 4285−4294.

(17) Bax, A.; Summers, M. F. ^{1}H and ^{13}C assignments from sensitivity-enhanced detection of heteronuclear multiple-bond connectivity by 2D multiple quantum NMR. *J. Am. Chem. Soc.* **1986**, *108*, 2093−2094.

(18) Schwarzenbach, R. P.; Stierli, R.; Folsom, B. R.; Zeyer, J. Compound properties relevant for assessing the environment partitioning of nitrophenols. *Environ. Sci. Technol*. **1988**, *22*, 83−92.

(19) Shishido, T.; Ohkawa, H. In *Methods in Pesticide Science;* Fukami, J., Uesugi, Y., Ishizuka, K., Tomizawa, C., Eds.; Soft Science: Tokyo, 1981; Chapter 1, pp 1−67.

(20) Weber, H.; Khorana, H. G. Polynucleotides. CIV. Total synthesis of the structural gene for an alanine transfer ribonucleic acid from yeast. Chemical synthesis of an icosadeoxynucleotide corresponding to the nucleotide sequence 21 to 40. *J. Mol. Biol*. **1972**, *72*, 219−249.

(21) Zhdanov, R. I.; Zhenodarova, S. M. Chemical methods of oligonucleotide synthesis. *Synthesis* **1975**, *4*, 222−245.

(22) Grindley, T. B. Structure and conformation of carbohydrate. In *Glycoscience Chemistry and Chemical Biology I*; Fraser, B., Tatuska, K., Thiem, J., Eds.; Springer: Berlin, 2001; Chapter 1, pp 33−41.

(23) Katagi, T. Molecular orbital approaches to the photolysis of organophosphorus insecticide fenitrothion. *J. Agric. Food. Chem.* **1989**, *37*, 1124−1130.

(24) Schwack, W.; Andlauer, W.; Armbruster, W. Photochemistry of parathion in the plant cuticle environment: model reaction in the presence on 2-propanol and methyl 12-hydroxyesterate. *Pestic. Sci.* **1994**, *40*, 279−284.

(25) Schynowski, F.; Schwack, W. Photochemistry of parathion on plant surfaces: relationship between photodecomposithion and iodine number of the plant cuticle. *Chemosphere* **1996**, *33* (11), 2255−2262.

(26) Eto, M. Chemical reactions. *Organophosphorus Pesticides: Organic and Biological Chemistry*; CRC Press: Cleveland, 1974; Chapter 3, pp 57−124.

(27) Ali, E. R.; Hopkins, T. L. Parathion absorption, translocation, and conversion to paraoxon in bean plants. *J. Agric. Food. Chem.* **1966**, *14*, 588−592.
(28) Chiba, M.; Kato, S.; Yamamoto, I. Metabolism of Cyanox and Surecide in bean plants and degradation in soil. *J. Pestic. Sci.* **1976**, *1*, 179−191.
(29) Stiasni, M.; Deckers, W.; Schmidt, K.; Simon, H. Translocation, penetration, and metabolism of *O*-(4-bromo-2,5-dichlorophenyl)-*O*,*O*-dimethylphosphorothioate (Bromophos) in tomato plants. *J. Agric. Food Chem.* **1969**, *17*, 1017−1020.
(30) O'Toole, J. C.; Cruz, R. T.; Seiber, J. N. Epicuticular wax and cuticular resistance in rice. *Physiol. Plant.* **1979**, *47*, 239−244.
(31) Baker, E. A.; Hunt, G. M. Developmental changes in leaf epicuticular waxes in relation to foliar penetration. *New Phytol.* **1981**, *88*, 731−747.
(32) Sen, A. Chemical composition and morphology of epicuticular waxes from of *Solanum tuberosum*. *Z. Naturforsch.* **1987**, *47c*, 1153−1158.
(33) Baker, E. A.; Bukovac, M. J.; Hunt, G. M. Composition of tomato fruit cuticle as related to fruit growth and development. *Linn. Soc. Symp. Ser.* **1982**, *10*, 33−44.
(34) Robert, D. B.; Sylvia, M. B.; Young, E.; Ross, B. L. Composition and variability of epicuticular waxes in apple cultivars. *J. Am. Soc. Hortic. Sci.* **1998**, *123* (3), 348−356.
(35) Bianchi, G. Plant Waxes. In *Chemistry, Molecular Biology and Functions*; Hamilton, R. J., Ed.; The Oily Press: Dundee, Scotland, 1995; Vol. 6, Chapter 5, pp 175−222.
(36) Katagi, T.; Mikami, N. Primary Metabolism of Agrochemicals in Plants. In *Metabolism of Agrochemicals in Plants*; Roberts, T., Ed.; Wiley & Sons: New York, 2000; Chapter 3, pp 43−106.
(37) Weston, L. A.; Barrett, M. Tolerance of tomato and bell pepper to clomazone. *Weed Sci.* **1989**, *37*, 285−289.
(38) Harvey, J., Jr.; Han, J. C. Y.; Reiser, R. W. Metabolism of oxamyl in plants. *J. Agric. Food Chem.* **1978**, *26* (3), 529−536.
(39) Preiss, U.; Wagner, K.; Oehlmann, L.; Engelhardt, G.; Wallnöfer, P. Metabolism of the insecticide baythroid by cell culture. *Chemosphere* **1984**, *13* (8), 861−872.
(40) Hodgson, R. H.; Frear, D. S.; Swanson, H. R.; Regan, L. A. Alteration of diphenamide metabolism in tomato by ozone. *Weed Sci.* **1973**, *21* (6), 542−549.
(41) Mikami, N.; Baba, Y.; Katagi, T.; Miyamoto, J. Metabolism of the synthetic pyrethroid fenpropathrin in plants. *J. Agric. Food Chem.* **1985**, *33*, 980−987.
(42) Malcherek, K.; Breuer, J.; Schuphan, I.; Schmidt, B. Metabolism of 4-nitrophenol in aspetically cultivated plants of the species wheat (*Triticum aestivum* L.), soybean (*Glycine max* L.), wild oat (*Avena fatus* L.) and corn cockle (*Agrostemma githago* L.). *J. Plant Physiol.* **1998**, *153*, 192−199.

Received for review March 25, 2003. Revised manuscript received June 5, 2003. Accepted June 9, 2003.

JF034289Q